Thermodynamic properties of triangle-well fluids in two dimensions: MC and MD simulations

Yuri Reyes, Mariana Bárcenas, Gerardo Odriozola, and Pedro Orea

Citation: The Journal of Chemical Physics **145**, 174505 (2016); doi: 10.1063/1.4967254
View online: https://doi.org/10.1063/1.4967254
View Table of Contents: http://aip.scitation.org/toc/jcp/145/17
Published by the American Institute of Physics

Thermodynamic properties of triangle-well fluids in two dimensions: MC and MD simulations

Yuri Reyes,[1,a)] Mariana Bárcenas,[2] Gerardo Odriozola,[3] and Pedro Orea[4]
[1]*Departamento de Recursos de la Tierra, Universidad Autónoma Metropolitana Unidad Lerma (UAM-L), Av. Hidalgo 46, Col. La Estación, CP 52006 Lerma de Villada, Mexico*
[2]*División de Ingeniería Química y Bioquímica, Tecnológico de Estudios Superiores de Ecatepec, CP 50210 Ecatepec, Mexico*
[3]*Área de Física de Procesos Irreversibles, División de Ciencias Básicas e Ingeniería, Universidad Autónoma Metropolitana (UAM-A), Av. San Pablo 180 Col. Reynosa, CP 02200 México D.F., Mexico*
[4]*Instituto Mexicano del Petróleo, Dirección de Investigación en Transformación de Hidrocarburos, Eje Central Lázaro Cárdenas 152, CP 07730 México D.F., Mexico*

(Received 15 June 2016; accepted 24 October 2016; published online 7 November 2016)

With the aim of providing complementary data of the thermodynamics properties of the triangular well potential, the vapor/liquid phase diagrams for such potential with different interaction ranges were calculated in two dimensions by Monte Carlo and molecular dynamics simulations; also, the vapor/liquid interfacial tension was calculated. As reported for other interaction potentials, it was observed that the reduction of the dimensionality makes the phase diagram to shrink. Finally, with the aid of reported data for the same potential in three dimensions, it was observed that this potential does not follow the principle of corresponding states. *Published by AIP Publishing.* [http://dx.doi.org/10.1063/1.4967254]

INTRODUCTION

Computer simulation of fluids is able to provide a deeper understanding of such systems. In order to properly model the behavior of real fluids, the employed potential should be as realistic as possible, while remain mathematically simple. The Lennard-Jones potential (LJP) model closely describes the interaction between neutral atoms or molecules because it takes into account the Pauli repulsion and van der Waals attraction. Although it is a mathematically simple potential capable of reproducing the behavior of noble gases (for example), its implementation in computer simulations is not free of difficulties, mainly due to the long attractive tail; to avoid such issues, some special treatments have been included in computer simulations.[1] On the other hand, finite potentials have received special attention not only because they can be implemented somehow easier in computer simulations but also because some of them can reproduce the behavior of real fluids and colloidal dispersions and can be used as a first attempt to develop theoretical approaches. One of the most studied finite potentials is the square-well potential (SWP), which contains a repulsive hard-core and a square attractive part that defines the interaction range. Plenty of thermodynamic properties have been calculated for the SWP in three dimensions (3D)[2,3] and two dimensions (2D).[4–6] Another potential with defined interaction range is the triangular-well potential (TWP) that also has a repulsive hard-core and its defined attractive well linearly goes to zero as the distance increases; this potential seems to be a closer representation of the LJP. The TWP has been studied for long time[7–10] receiving renewed attention in recent publications.[11–15] However, there is a lack of information about some of the thermodynamic properties of the TWP. Specifically, to the best of the authors' knowledge, there is no information about the thermodynamic properties of the TWP in two dimensions, which is available for other model potentials. Studying the thermodynamics properties of fluids in two dimensions is relevant to know the effect of the reduction of the dimensionality on the thermodynamic properties of the fluids modeled by the TWP and also because some real systems can be considered as 2D fluids, such as surfactants and colloids adsorbed on an air/water interface or monolayers adsorbed on solid substrates[16] among other systems.[17]

The objective of the present contribution is to complement the available information of the TWF by providing simulation results of the vapor/liquid (VL) phase diagram and VL interfacial tension in 2D for different interaction ranges. To calculate the thermodynamic properties, Monte Carlo (MC) and Molecular Dynamics (MD) simulations were carried out.

SIMULATION DETAILS

The TWP, u(x), is given by the following equation:

$$u(x) = \begin{cases} \infty & \text{for} \quad x < 1 \\ \epsilon\,(x-\lambda)/(\lambda-1) & \text{for} \quad 1 \le x \le \lambda \\ 0 & \text{for} \quad \lambda < x \end{cases}, \qquad (1)$$

where $x = r/\sigma$ is the dimensionless distance between particles (given by r), in which σ is the hard-core diameter (σ is the unit of length), ε is the potential well depth, and λ is the interaction range. Dimensionless units are defined as $T^* = k_B T/\varepsilon$ for temperature (k_B is the Boltzmann constant), $\rho^* = \rho\sigma^2$ for number density, and $\gamma^* = \gamma\sigma/\varepsilon$ for the interfacial tension. The

a)Author to whom correspondence should be addressed. Electronic mail: yuri.reyes.mx@gmail.com

interaction ranges studied in this contribution are λ = 2.25, 2.50, 3.00, 3.50, and 4.00.

The vapor/liquid phase diagram of the TWP in 2D was calculated by Monte Carlo (MC) and Molecular Dynamics (MD) simulations in the canonical ensemble, by using a rectangular simulation box with lengths $L_x = 90$ and $L_y = 40$, with periodic boundary conditions in both directions and 1200 particles in all simulations. For MC simulations, the particles were initially inserted at random in the simulation box for each temperature; the system was left to equilibrate for 10^7 MC configurations according to the Metropolis algorithm, with an acceptance ratio of 30%. Density profiles through the x-axis were recorded in 10 blocks of 10^6 MC additional configurations. Then the average of the density profiles was used to determine the liquid-like and vapor-like densities.

Since the TWP is a discontinuous potential; to carry out MD simulations, a constant-force approach was used to deal with the hard core repulsion. Briefly, the discontinuity of the potential is approached by a linear function with a negative slope α which results in a constant repulsive force acting on overlapping particles.[18] To provide a good approximation, α must be such that the radial distribution function evaluated at x = 0.99 should be less than 10^{-4}, which works quite well for other potentials. The higher the temperature the higher the value of the slope α to keep a low degree of overlap, hence α is increased when dealing with larger interaction ranges, since the critical temperature is larger. This approach provides very similar results to MC simulations of the TWP in three dimensions;[13] this fact will also be studied in the present contribution and, importantly, it allows an easy calculation of the vapor/liquid surface tension, γ, by MD simulations through the virial route, by using the following equation:

$$\gamma = \frac{L_x}{2}\left\{\langle P_{xx}\rangle - \langle P_{yy}\rangle\right\}, \tag{2}$$

in which P_{ii} are the diagonal components of the pressure tensor (in units of force per unit length in 2D) and L_x is the length of the simulation box normal to the interface. The brackets denote the ensemble average.

The MD simulations were carried out with HOOMD-blue.[19] The constant integration step was 0.0002 dimensionless units. Since the open source code allows the use of tabulated potentials, to calculate the VL phase diagram and the diagonal components of the pressure tensor, for λ = 2.25 and 2.5 a slope of α = 400 was used, whereas for λ = 3.00, 3.50, and 4.00, α = 800. For each temperature, the particles were inserted at random in the simulation box and the system was left to equilibrate for 2×10^8 dimensionless time steps; the reported results come from analyzing of the trajectories generated in posterior 10^9 time steps, to calculate the density profiles and the diagonal components of the pressure tensor.

The critical properties, T^*_c and ρ^*_c were obtained with the rectilinear diameters law and the scaling relationship with the universal value of β = 0.325.[3]

RESULTS AND DISCUSSION

To begin with the analysis, the vapor/liquid (VL) phase diagram for different interaction ranges obtained by MC and MD simulations is shown in Figure 1. The behavior of the phase diagram of the TWP in 2D shows that for the largest interaction range considered in the present study, λ = 4.00, the VL is the widest along with the highest critical temperature. As the interaction range decreases, the VL coexistence curve shrinks and the critical temperature decreases. This makes the vapor to become more dense as λ diminishes and, in contrast, the liquid to become less dense. It should be noted that for λ = 2.25 (the lowest interaction range considered in this work) the VL coexistence curve is presented in a narrow temperature range. Actually, it was not possible to obtain the VL envelope for lower values of λ with the employed methodology. The behavior of the VL phase diagram of the 2D-TWP is similar to the three dimensional system[11,13] but, for all interaction ranges, the critical temperature is lower for the 2D than for 3D systems. For example, for λ = 2.5 the critical temperature is ca. 0.82 and 2.11 for 2D and 3D, respectively, and for λ = 4.0 the critical temperature is 2.05 and 7.50 for 2D and 3D, respectively. Such reduction of the critical temperature of the 2D systems has been observed for other potentials, i.e., LJP[17] and SWP.[20,21] On the other hand, it can be seen that between both simulation techniques, MC and MD simulations, the results show reasonable agreement, considering that MC simulations were carried out with a home-made Fortran code and MD with an open source code. The largest disagreement is shown in the low temperature of the VL diagram of λ = 3.00 and 3.50. Perhaps longer simulation runs are required to obtain a better match between the two simulation techniques.

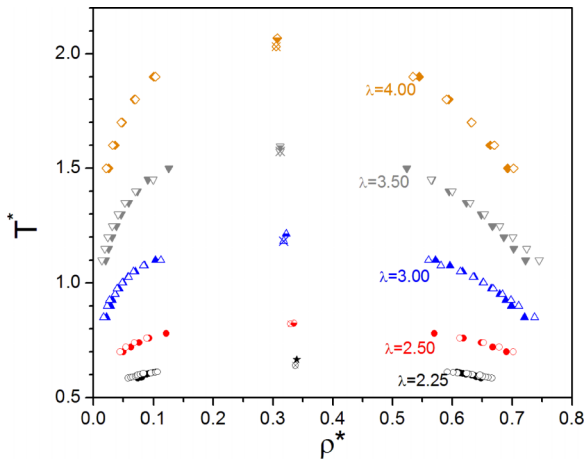

FIG. 1. Equilibrium vapor/liquid phase diagram for the TWP in 2D for different interaction ranges. Filled symbols correspond to MC simulations, whereas empty symbols correspond to MD simulations. The critical point from MC simulations is depicted by a crossed empty symbol and with a half filled symbol for MD simulations.

Due to the rather good agreement of the values of the equilibrium densities calculated by MC and MD, it is expected to have also a good agreement of the critical properties, T^*_c and ρ^*_c, which are analyzed as a function of the interaction range in Figure 2. It can be seen that the critical properties calculated by the two simulation techniques are nearly overlapped. The top panel of Figure 2 shows that the critical temperature increases as the interaction range does, whereas the critical density decreases (bottom panel). In the same figure, the critical data for some interaction ranges of the TWP in 3D are

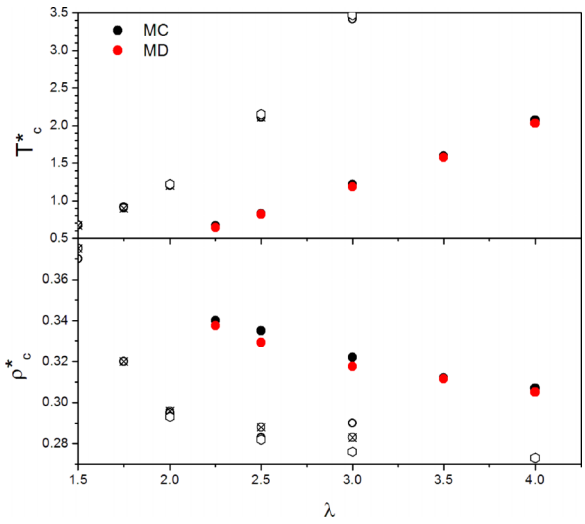

FIG. 2. Critical temperature (top panel) and critical density (bottom panel) calculated from the VL phase equilibrium results by both MC (black circles) and MD (red circles) simulations for the TWP in 2D. Critical parameters for the three dimensional systems are included: empty circles and crossed circles from Ref. 13 obtained by MC and MD, respectively; empty hexagons from Ref. 11.

also included for comparison. If we compare the data for 2D and 3D, it is observed that the T^*_c of the TWP in 3D is higher than the one in 2D, as discussed above. On the other hand, the critical density for 3D is lower than for the 2D case. For both critical parameters, the interval of variation is lower for the 2D consideration. The critical density of the TWP in both dimensions decreases monotonically as the interaction range increases. This result is relevant since it has been demonstrated that the critical density has an oscillatory behavior when analyzed as a function of the interaction range for the square-well potential in both dimensions.[6] This oscillatory behavior might be artificial for real fluids, making the TWP to be a closer model for actual interparticle interactions.

Another important parameter is the second virial coefficient, which could be used to develop equations of the state and it is a measurement of the relative importance of the attractive/repulsive interactions, i.e., a more positive value of the second virial coefficient indicates that repulsion is dominant and vice versa.[6] The second virial coefficient in 2D, $B_2(T)$, is defined by[22,23]

$$B_2(T) = \pi \int_0^\infty \left(1 - \exp\left(-U(r)/T\right)\right) r dr, \tag{3}$$

which is solved analytically to give

$$B_2(T) = \pi \left[\frac{\sigma^2}{2} + \frac{1}{2}\left(\lambda^2 - \sigma^2\right) - (\lambda - \sigma)\left(\sigma e^{1/T} - \lambda\right) T + (\lambda - \sigma)^2 \left(1 - e^{1/T}\right) T^2 \right]. \tag{4}$$

$B_2(T)$ can be reduced by $B_{2,HD} = \pi\sigma^2/2$, which is the second virial coefficient of hard discs, to get the reduced second virial coefficient, $B^*_2(T) = B_2(T)/B_{2,HD}$. Figure 3 shows the behavior of the reduced second virial coefficient evaluated at T^*_c using the calculated results for 2D systems and the reported ones for the 3D systems. For the 2D systems, it can be observed that the value of $B^*_2(T^*_c)$ increases as a function of the interaction range and then it keeps growing with a lower slope, whereas for the 3D system the reduced second virial coefficient remains nearly constant.

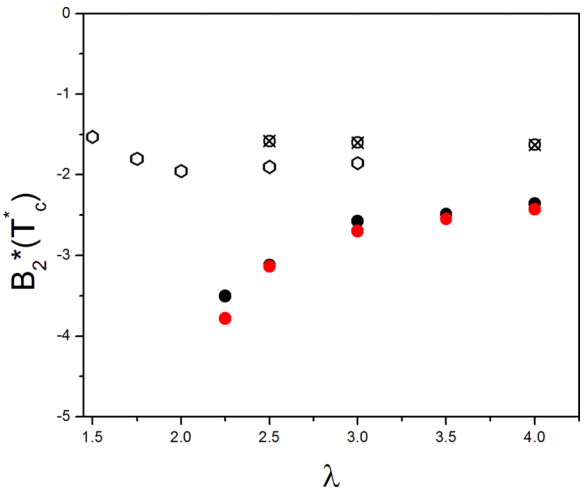

FIG. 3. Reduced second virial coefficient, $B^*_2(T^*_c)$, as a function of the interaction range. Filled symbols correspond to 2D simulations (black for MC and red for MD) and empty symbols to 3D, with the same meaning as in Figure 2.

The new results of the interfacial tension of the 2D system are presented in Figure 4. As is the case for other potentials, the higher the temperature the lower the interfacial tension until the critical temperature is reached, at which the interfaces vanish. Additionally, as is the case for other interaction potentials, the larger the interaction range the higher the interfacial tension at a given temperature. Data for $\lambda = 2.25$ are not shown due to the large relative error; therefore, it is not possible to use the proposed approach to calculate the interfacial tension for this short interaction range. Moreover, the values of the surface tension of the TWF in 2D are lower than the ones for the fluid in three dimensions for the same interaction range. For example, for $\lambda = 2.50$ the largest interfacial tension (calculated in this contribution) is around 0.25 for the 2D, while for the 3D is around 3.00.[13]

Finally, the equilibrium data of the TWF in 2D and 3D were analyzed to observe if this potential follows the law

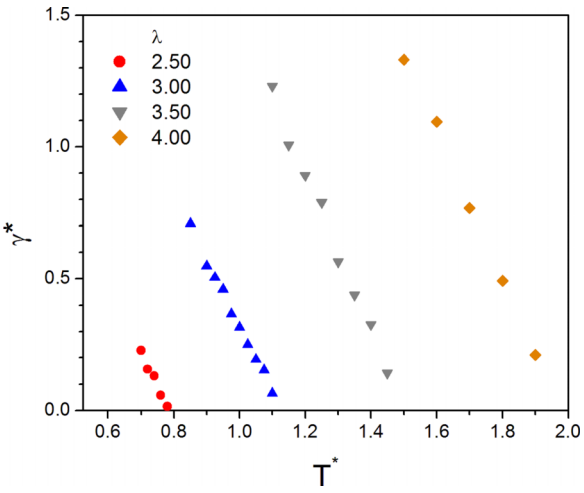

FIG. 4. Interfacial tension of the TWP in 2D as a function of temperature for different interaction ranges.

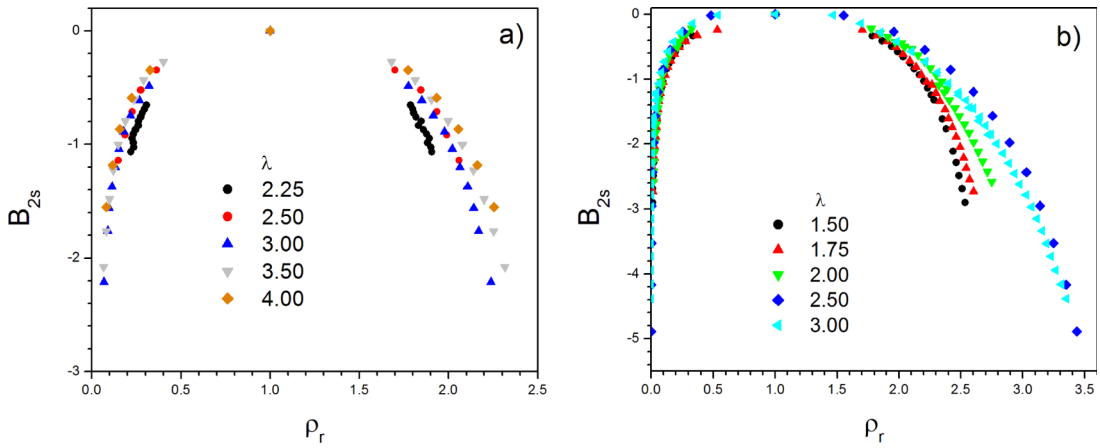

FIG. 5. VL diagrams in terms of $B_{2s} = B_2^*(T^*) - B_2^*(T_c^*)$, for (a) 2D using MD data and (b) 3D using MD data from Ref. 9. All data come from molecular dynamics results. Note that in these graphs, B_{2s} has replaced the temperature. It can be observed that there is not a collapse of the diagrams of the TWP.

of corresponding states, but instead of using the reduced temperature, ($T^*_r = T^*/T^*_c$), the VL properties were analyzed in terms of the difference between the reduced second virial coefficient evaluated at each temperature and the one evaluated at the critical temperature, $B_{2s} = B_2^*(T^*) - B_2^*(T_c^*)$, which has been applied to analyze the results of Mie, Yukawa, square-well,[24] and Lennard-Jones potentials.[25] It has been observed that most of the VL properties of these potentials collapse to form a single master curve when analyzed in terms of B_{2s} instead of the reduced temperature. For the SWP, there are two curves in which the VL properties collapse. The results of Figure 5 for the TWP in two and three dimensions show that the TWP potential does not follow the law of corresponding states in both 2D and 3D because the curves do not collapse to yield a master curve, instead there is a gradual displacement. For the SWP, the presence of two groups of curves was related to the formation of primary and secondary coordination shells at a given interaction range;[24] however, in the TWP the situation is different because although it is a finite potential, the attractive well linearly tends to zero, making the primary coordination shell (and the subsequent ones) to be fuzzy. This is why, we think that the TWP is transiting from a kind of SWP short-range behavior to a SWP long-range one. We lack a fundamental explanation for this behavior, though.

CONCLUSIONS

The vapor/liquid phase diagrams of the TWP in two dimensions were calculated by MC and MD simulations. The results obtained by the two simulation approaches are in good agreement among them. The observed behavior of the TWP VL diagram is similar to the one obtained for other potentials with defined interaction range, i.e., the larger the interaction range, the higher the critical temperature and the wider the VL envelope and as the interaction range decreases, the VL coexistence curve shrinks. It was also observed that the critical temperature of the TWP in 2D is lower as compared to the 3D system, but the critical density is greater in 2D than in 3D. This feature is common with other potentials. Regarding the reduced second virial coefficient evaluated at T^*_c, it shows a decreasing behavior in 2D as the interaction range increases. Also, new results of the interfacial tension were presented. Finally, it was observed that the TWP does not follow the law of corresponding states, when instead of using the reduced temperature the analysis is done by using B_{2s} which works for other potentials.

ACKNOWLEDGMENTS

The authors would like to thank CONACyT-México for financial support. P.O. acknowledges D.61017 from IMP-México. This work was developed in the cluster Axolotl at UAM-L.

[1]A. Trokhymchuck and J. Alejandre, J. Chem. Phys. **111**, 8510 (1999).
[2]P. Orea, Y. Duda, and J. Alejandre, J. Chem. Phys. **118**, 5635 (2003).
[3]R. López-Rendón, Y. Reyes, and P. Orea, J. Chem. Phys. **125**, 084508 (2006).
[4]H. L. Vörtler, K. Schäfer, and W. R. Smith, J. Phys. Chem. **112**, 4656–4661 (2008).
[5]Y. Reyes, C. A. Flores-Sandoval, and P. Orea, J. Chem. Phys. **139**, 164505 (2013).
[6]J. C. Armas-Pérez, J. Quintana-H, G. A. Chapela, E. Velasco, and G. Navascués, J. Chem. Phys. **140**, 064503 (2014).
[7]T. Nagayima, Proc. Phys.-Math. Soc. Jpn. **22**, 705–720 (1940).
[8]M. J. Feinberg and A. D. De Rocco, J. Chem. Phys. **41**, 3439–3450 (1964).
[9]W. C. Farrar and A. G. De Rocco, J. Chem. Phys. **54**, 2024–2025 (1971).
[10]W. R. Smith, D. Henderson, and J. A. Barker, Can. J. Phys. **53**, 5–12 (1975).
[11]F. F. Betancourt-Cárdenas, L. A. García-Luna, A. L. Benavides, J. A. Ramírez, and E. Schöll-Paschinger, Mol. Phys. **106**, 113–126 (2008).
[12]L. D. Rivera, M. Robles, and M. López de Haro, Mol. Phys. **110**, 1317–1323 (2012).
[13]M. Bárcenas, G. Odriozola, and P. Orea, Mol. Phys. **112**, 2114–2121 (2014).
[14]A. Sengupta, P. Behera, and J. Adhikari, Mol. Phys. **112**, 1969–1978 (2014).
[15]A. Sengupta and J. Adhikari, Chem. Phys. **469-470**, 16–24 (2016).
[16]B. Smit and D. Frenkel, J. Chem. Phys. **94**, 5663–5668 (1991).
[17]M. R. Eustaquio-Armenta, G. A. Méndez-Maldonado, and M. González-Melchor, J. Chem. Phys. **144**, 134705 (2016).
[18]P. Orea and G. Odriozola, J. Chem. Phys. **138**, 214105 (2013).
[19]J. A. Anderson, C. D. Lorenz, and A. Travesset, J. Comput. Phys. **227**, 5342–5359 (2008).
[20]J. C. Armas-Pérez, J. Quintana, and G. A. Chapela, J. Chem. Phys. **138**, 044508 (2013).
[21]W. Rzysko and A. Trokhymchuk, J. Chem. Phys. **137**, 224505 (2012).
[22]J. E. Krizan and A. D. Crowell, J. Chem. Phys. **41**, 1322–1326 (1964).
[23]I. D. Morrison and S. Ross, Surf. Sci. **39**, 21–36 (1973).
[24]P. Orea, S. Varga, and G. Odriozola, Chem. Phys. Lett. **631-632**, 26–29 (2015).
[25]P. Orea, A. Romero-Martínez, E. Basurto, C. A. Vargas, and G. Odriozola, J. Chem. Phys. **143**, 024504 (2015).